Computing and Informatics, Vol. 40, 2021, 1398–1421, doi: 10.31577/cai_2021_6_1398

IMAGE ENHANCEMENT ALGORITHM BASED ON IMAGE SPATIAL DOMAIN SEGMENTATION

Tianhe Yu, Ming Zhu

Harbin University of Science and Technology
School of Measurement and Communication Engineering
Harbin 150080, China
e-mail: ythaa@163.com

Abstract. This paper proposes an image enhancement algorithm based on the theory of image segmentation and image frequency. First, a mathematical model corresponding to the pixel frequency is established by using the difference of pigment values between the pixels in the image and the surrounding pixels (i.e., pixel receptive field). Then, the image is divided into the low frequency region (background area), low-medium frequency region (foreground area), medium-high frequency region (target area) and high frequency region (detail area) by a pixel frequency characteristic graph. Gamma correction, MSRCR, MSR, top hat + bottom hat are used for image enhancement for each area, and then the parts are merged. Three indicators of PSNR, SSIM, and MSE are introduced to evaluate the quality of the enhanced image. The results show that the image enhanced by this algorithm has the highest PSNR and SSIM values and the lowest MSE value, indicating that the enhancement effect of this algorithm is better. Compared with traditional algorithms, the image enhancement algorithm in this paper produces higher image quality and richer details.

Keywords: Mathematical model, frequency characteristics, regional segmentation, image enhancement

Mathematics Subject Classification 2010: 68-U10

1 INTRODUCTION

Image processing is crucial to applications including face recognition and fingerprint unlocking, as well as in operational engineering fields such as detecting the terrain of a specific area. In these applications, image enhancement technology plays a critical role to enable faster and more accurate identification and information extraction. The improvement of image enhancement technology can also greatly improve the quality of the target image, and generate details when the image quality is poor. Enhancement methods mainly include gamma correction, as well as methods based on histograms, wavelets and Retinex [1].

The new image enhancement algorithm is based on Retinex theory [2, 3], which can estimate the environmental component according to the image area, and eliminate the influence of environmental light component to obtain the reflection component. The algorithm is divided into three parts: center surround, random path, and homomorphic filtering [4], with the central surround algorithm being the most representative algorithm. Traditional algorithms include single scale Retinex (SSR) [5], multi-scale Retinex (MSR) [6] and multi-scale Retinex with color restoration (MSRCR) [7]. At present, the image enhancement algorithm based on Retinex theory still needs to be improved: first, halos are easily generated in the area where the light and shade of the image change dramatically; second, the noise in the area is amplified due to the over enhancement of the dark areas in the image; third, the pixel overflowing in the bright area of the image results in the loss of detailed information; finally, as the number of parameters is large and different parameters are set for specific images, the algorithm has poor adaptability.

Wang et al. [8] proposed an improved algorithm for adaptive infrared image enhancement based on guided filtering, which can highlight detail contour information and reduce the influence of detail layer noise on the output image after fusion. Han et al. [9] proposed an improved Retinex-based estimation method for the illumination map, which achieves image enhancement by combining L2 norm and Gamma correction. Lan et al. [10] proposed an image enhancement algorithm based on adaptive intuitionistic blur and different histogram cropping, which used the hesitation of the intuitionistic fuzzy set to describe the unknown information of the original image and correct the detailed image obtained by the guided filtering. Cao et al. [11] proposed an adaptive non-uniform low-illuminance image enhancement algorithm by combining the Retinex algorithm with the principal component analysis method. Cai et al. [12] combined the fuzzy domain with the homomorphic filtering method through the HSV color space, and proposed a color image enhancement algorithm based on fuzzy homomorphic filtering to enhance the image and reduce the computational complexity.

The existing image enhancement algorithm usually performs well on a specific frequency domain or spatial domain image such as the detail of the image. One of the advantages of the enhancement algorithm is that the whole image can be saved. The image details are considered to the high-frequency component when the frequency is changed, and the image frequency of the image is distributed in the low

frequency area. The image enhancement algorithms that currently exist only work well for a certain kind of image and adapt poorly to a wide range of images. When an image is collected and transmitted, issues such as image noise, insufficient or uneven illumination and brightness are inevitably prevalent. High frequency regions such as the edge of the image will also be lost during image processing when traditional algorithms are used. To mitigate these problems, we have developed a reliable and adaptive image enhancement algorithm which can achieve image enhancement and processing at the same time.

2 BASIC THEORIES

2.1 Frequency Division Theories

Human eyes have different visual characteristics [13, 21] to machines, according to which vision can be divided into different sensitive regions. Figure 1 reflects the relationship between the contrast threshold and the luminance.

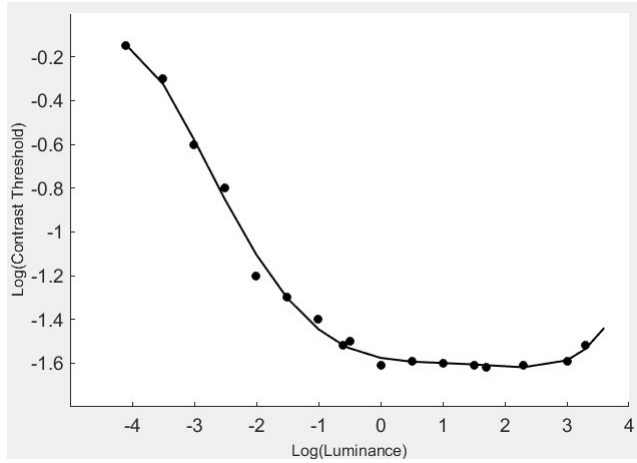

Figure 1. Graph of the relationship between contrast threshold and luminance

In the low brightness state, log(*Luminance*) is less than 0, and the contrast threshold is inversely proportional to the square root of the brightness, which obeys the DeVries-Rose law [13]. As the brightness increases, log(*Luminance*) is between 0–3, and the contrast threshold is constant, which obeys the Weber law. In the state where log(*Luminance*) is greater than 3, it is a saturated area and is considered a high-brightness area.

2.2 Gaussian Kernel Function

The following Equation (1) is a two-dimensional Gaussian kernel function [14]:

$$G(x,y) = \frac{1}{2\pi\sigma^2}\exp\left(-\frac{(x-x_0)^2+(y-y_0)^2}{2\sigma^2}\right) \tag{1}$$

where (x, y) is the coordinates of the space point, (x_0, y_0) is the position of the space center point, σ is the standard deviation and G is the weighted value corresponding to (x, y) points. The Gaussian function image is shown in Figure 2.

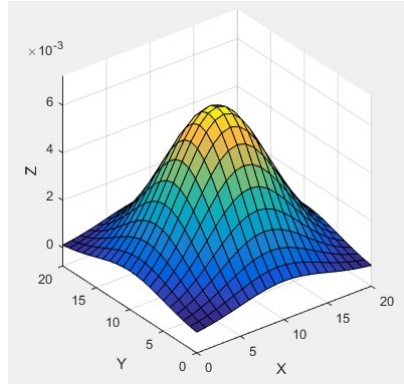

Figure 2. Gaussian kernel function plot

The parameters of the Gaussian convolution kernel are defined as follows:

$$\begin{bmatrix} 0.0751136 & 0.123841 & 0.0751136 \\ 0.123841 & 0.20418 & 0.123841 \\ 0.075113 & 0.123841 & 0.0751136 \end{bmatrix}.$$

The Gaussian convolution kernel template is used to convolute the variance matrix of the image. The center point on the template coincides with the center point in the matrix, and the two values of the corresponding points are multiplied so that each weight value contains the distance value from the center point. The influence on the center point is directly proportional to the distance and inversely proportional to the impact force and mass. The standard deviation in the mathematical concept is used to measure the disturbance frequency of the pixel value in the receptive field of the pixel point, and the frequency of the pixels in the image is determined one by one. In order to highlight the influence of the weighting of the value of the central point pixel on the overall receptive field, the proportion of variance data in the overall evaluation is set, and the variance proportions in the overall evaluation are adjusted to make the total proportion equal to 1. All numbers are then summed by their weighted product. In this paper, a 3×3 Gaussian convolution kernel is selected to calculate the frequency measurement value at the center point.

2.3 Image Enhancement Algorithms

2.3.1 Gamma Correction Enhancement

The algorithm [15, 16] is as follows:

1. **Normalization:** transporting the pixel value to a real number between 0 and 1. $(I + 0.5)/256$ here includes a division and an addition operation. For the pixel a, the corresponding normalization value is 0.783203.
2. **Pre-compensation:** from Equation (1), the corresponding value of the normalized pixel data is calculated with 1/gamma as the index. In this step, the calculation involves an exponential operation. When the gamma value is 2.2, 1/gamma = 0.454545. Thus, the result of pre-compensation for the normalized value A is $0.7832030.454545 = 0.894872$.
3. **Denormalization:** taking the inverse of a pre-compensated real value to obtain an integer value between 0 and 255. The specific algorithm is: $f \cdot 256 - 0.5$. This step includes a multiplication and a subtraction operation. The enhanced effect is shown in Figure 3.

a) Original image b) Gamma correction enhancement image

Figure 3. Comparison of the a) original image and b) the enhanced image through the Gamma correction

2.3.2 Multi-Scale Retinex Enhancement

In the SSR algorithm, the size of the filtering scale affects the quality of processed image directly. Defects such as color distortion and halos may appear in the processed image when it is small otherwise, and the compression effect of the image is poor in the dynamic range. To balance dynamic range compression and color fidelity, the Retinex algorithm at different scales is weighted linearly, generating the multi-scale Retinex (MSR) [17] algorithm.

$$r_i = \log[R_i(x, y)] \tag{2}$$

where $R_i(x, y)$ is the reflection component of the corresponding channel. The output formula for the MSR algorithm is as follows:

$$r_i = \sum_{k=1}^{K} W_k \{\log[S_i(x, y)] - \log[S_i(x, y) \cdot G_k(x, y)]\} \tag{3}$$

where the original image of the corresponding scale is $S(x, y)$. The R, G and B are the three color channels and i is a parameter with values of 1, 2 and 3. The parameter k represents the number of scales of MSR algorithm. A larger value results in a sharper image, but also increases the duration of computation. Generally, $k = 3$, $W_1 = W_2 = W_3 = 1/3$, where W_k refers to the weighted value at the k^{th} scale. This gives rise to the following formula:

$$\sum_{k=1}^{K} W + k = 1 \tag{4}$$

where W_k represents the Gaussian function at the k^{th} scale, and the mathematical formula is as follows:

$$G_k(x, y) = -\frac{1}{\sqrt{2\pi}\sigma_k} \exp\left(-\frac{(x^2 + y^2)}{2\sigma_k^2}\right) \tag{5}$$

where σ_k represents the value of the k^{th} scale in MSR algorithm. Experiments have shown that the use of three standard scales (low, medium and high) can obtain good results. The reflection section of the image is obtained as follows:

$$R_i(x, y) = \exp(r_i). \tag{6}$$

The weighted average of the SSR algorithm obtains the MSR algorithm, which combines the advantages of filtering functions in different scales. Not only can it achieve the color fidelity of the processed image, the dynamic range of compression is also expanded. On the whole, the MSR image algorithm achieves better results as the dynamic range of compression is extended and the color fidelity of the image is preserved.

From the original image in Figure 4 a), it is evident that the light distribution is uneven and the brightness of the target object in the figure is low and difficult to observe by the human eye. After processing by MSR, the overall brightness of the image is improved, and the effect of object enhancement in the medium-high frequency range is good. However, the high frequency regions which depict contours of the target in the image become less obvious after MSR processing, and that leads to a decrease of the overall contrast of the image due to the improvement of the overall brightness of the target area. As such, the target area and the background area cannot be distinguished clearly, and is not easily observed by the human eye.

a) Original image b) MSR enhancement image

Figure 4. Comparison of the a) original image and b) the enhanced image through the MSR algorithm

2.3.3 Multi-Scale Retinex with Color Restoration Enhancement

In the MSR enhancement algorithm, the image will be distorted due to the increase of noise, which makes the color of the local details of the image distorted, and cannot show the true color of the object, resulting in poor visual effects. In response to this deficiency, Multi-scale Retinex with Color Restoration (MSRCR) [18] enhancement algorithm adds a color restoration factor to the MSR to adjust the color distortion caused by the contrast enhancement of the local area of the image. The algorithm is briefly described as follows:

1. Calculate the mean *Mean* and mean square deviation *Var* of each channel data in $\log[R(x, y)]$.
2. Calculate the minimum *Min* and maximum *Max* of each channel:

$$Min = Mean - Dynamic \cdot Var, \tag{7}$$

$$Max = Mean + Dynamic \cdot Var. \tag{8}$$

   where *Dynamic* is a dynamic adjustment parameter. The contrast of the image becomes stronger as the *Dynamic* value decreases. *Dynamic* generally takes a value between 2–3, which can not only achieve a natural transition effect, but also maintain a moderately enhanced image sharpness.
3. Perform a linear mapping for each value of $\log[R(x, y)]$:

$$R(x, y) = (Value - Min)/(Max - Min) \cdot (255 - 0). \tag{9}$$

Figure 5 below is a comparison between the original image and the image after MSRCR processing.

a) Original image b) MSRCR enhancement image

Figure 5. Comparison of the a) original image and b) the enhanced image through the MSRCR algorithm

It can be seen from the original image that the overall tone of the original image is dark, and the edges of the nearby background buildings are blurry, while the distant buildings are completely invisible, with low contrast and poor visual effects. After MSRCR processing, the overall image effect is brighter, the edges of nearby buildings are clearer, and the ships are also distinct in color. The sharpness of distant buildings is improved compared with the original image, but it is still not very clear. The overall image contrast has been greatly improved, making it easier to distinguish objects in the image.

2.3.4 Top Hat + Bottom Hat Enhancement

The top-hat [19] part i_{TOP} is obtained by the morphological opening operation and the bottom hat part i_{BOT} is obtained by morphological closing operation. The transition image t is obtained by adding the original image and the top hat part:

$$t = f + i_{TOP}. \tag{10}$$

Thus, the enhanced image is:

$$g = t - i_{BOT} = f + i_{TOP} - i_{BOT}. \tag{11}$$

The details of the image are enhanced to be clearer and the target object in the image is in the high-frequency region after image morphology processing. Image enhancement technology can enhance the target texture, edge features and brightness contrast to obtain clearer image details.

The first step involves the use of frequency segmentation technology to process the image, followed by image enhancement through this algorithm. Finally, the segmented image is used to obtain the enhanced image, shown in Figure 6.

a) Original image b) After enhancement

Figure 6. Comparison of the a) original image and b) the enhanced image through the top hat + bottom hat algorithm

3 IMAGE ENHANCEMENT ALGORITHM BASED ON SPATIAL FREQUENCY SEGMENTATION

Typically, an image is divided into four regions, although five or more detail regions may achieve better results in some cases, while the frequency measurement matrix can be used to calculate the frequency of the global pixel [20, 21]. The matrix is normalized to the range of 0–1, and then divided into four parts on average to calculate the mark matrix. The original image is divided into different frequency areas by using the marking matrix, such that the background and the foreground of the image are represented by the low frequency and the low-medium frequency respectively, while the objects of the image are determined by the medium-high frequency and the details of the image are represented by the high frequency.

In this paper, four sub-images are used to synthesize the image through the frequency segmentation technology. The algorithm structure block diagram is shown in Figure 7.

Simple linear iterative clustering (SLIC) [22, 23, 24] applies the k-means clustering principle to generate superpixels rapidly and efficiently. SLIC can obtain boundary information faster than the previous segmentation algorithms. The detailed implementation steps of SLIC are as follows: first, the number of superpixels to be segmented is initialized. Then, the seed pixel block is assigned and the surrounding pixel block is classified. The superpixel metric is then calculated and classified, and the threshold of the cluster pixel block center is determined. Finally, clustering is performed based on Equation (1). To assign a corresponding frequency value to each pixel of the original image, a mathematical model is proposed to transform the pixel value of image into the corresponding frequency space. In this study, 3×3

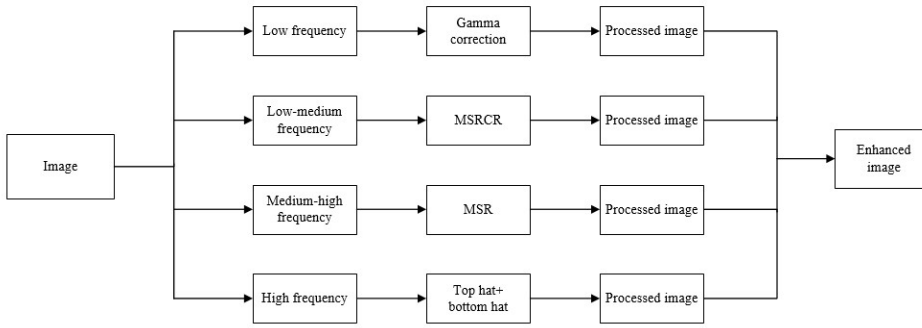

Figure 7. Algorithm structure block diagram

receptive field matrix is used to calculate the frequency of the center point. The mathematical model is obtained by calculating the variance of the pixel value in the receptive field region and determined by Gaussian kernel weighting. By using this method in comparison with the Gaussian convolution kernel where all weights are equal to 1, the influence of the center point is more prominent when the pixel value is in the boundary of the image. At the boundary, the pixel values in the receptive field range are added to the calculation, and the positions where the pixels exceed the range are not calculated. As a result, all the points on this image can be mapped to another space, and the standard deviation weighted by the Gaussian kernel is used as the measurement standard. The next step is to normalize the measurement matrix of the image to the range of 0–1. The area with median measurement matrix values is divided into 4 regions according to 0–0.25, 0.25–0.5, 0.5–0.75, and 0.75–1 through segmentation, corresponding to low, low-medium, medium-high and high frequency regions. The algorithm realization process is shown in Figure 8.

As discussed above, the image can be divided into four frequency ranges. In general, the low frequency and low-medium frequency regions respectively represent the background and the foreground of the image, while non-detailed parts are usually represented by the middle-high frequency region. The details of the image are represented by high frequency regions. To improve the feature clarity of the image, the brightness balance of the image needs to be adjusted. The gamma correction algorithm is used to process the low-frequency part of the image to increase the proportion of dark and light colors in the low-frequency area, thereby improving the contrast in the low-frequency area. Because the MSRCR algorithm has better color reproducibility, brightness constancy and dynamic range compression characteristics, MSRCR is used to deal with the low-medium frequency region. The MSR algorithm processes the medium-high frequency region, while maintaining the high fidelity of the medium-high frequency region. The final high-frequency region is processed using both top hat and bottom hat algorithm to correct the effects of uneven lighting. Combining the four algorithms. In this study, the Retinex algorithm

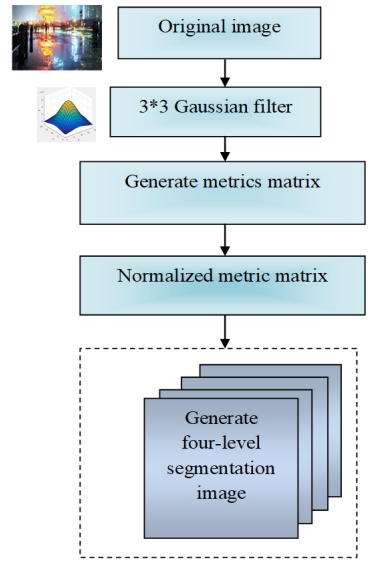

Figure 8. Weber's four-part segmentation algorithm

is used to counter problems arising from differences in brightness and developed an image edge enhancement algorithm based on image morphology and transformed by gamma correction, top hat and bottom hat.

In this paper, the RGB Three-Channel-Four-Region image segmentation is used, and the original images are shown in Figure 9.

a) Forest path b) Landscape c) Urban nightscape image

Figure 9. Original images

The results of the segmentation experiment are shown in Figure 10.

Note: As shown in Figure 10, there are three channels R, G and B in each picture. Then, the pictures of each channel are divided into four regions by the frequency mapping model algorithm of low frequency, low-medium frequency, medium-high frequency and high frequency. It is evident from Figure 10 that the background of the picture is primarily a low frequency area, and the foreground is a combination of

a1) Segmentation of low frequency

b1) Segmentation of low frequency

c1) Segmentation of low frequency

a2) Segmentation of low-medium frequency

b2) Segmentation of low-medium frequency

c2) Segmentation of low-medium frequency

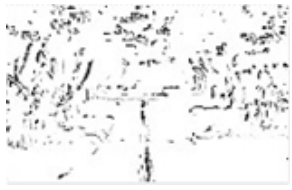

a3) Segmentation of medium-high frequency

b3) Segmentation of medium-high frequency

c3) Segmentation of medium-high frequency

a4) Segmentation of high frequency

b4) Segmentation of high frequency

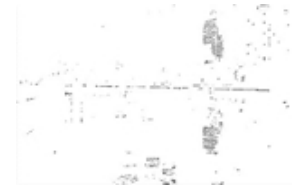

c4) Segmentation of high frequency

a) Forest path image b) Landscape image c) Urban nightscape image

Figure 10. Results of the segmentation experiment of R channel

the low-medium frequency areas, while the medium-high frequency constitutes the target area, and the details are distinguished by high frequency.

4 EXPERIMENTAL RESULTS AND ANALYSIS

In this experiment, three groups of pictures are used to evaluate the enhancement effect of the algorithm, and the results of the images of the forest path are shown in Figure 11. The enhanced images of the urban nightscape by different algorithms

are shown in Figure 12, while those of the landscape images are shown in Figure 13.

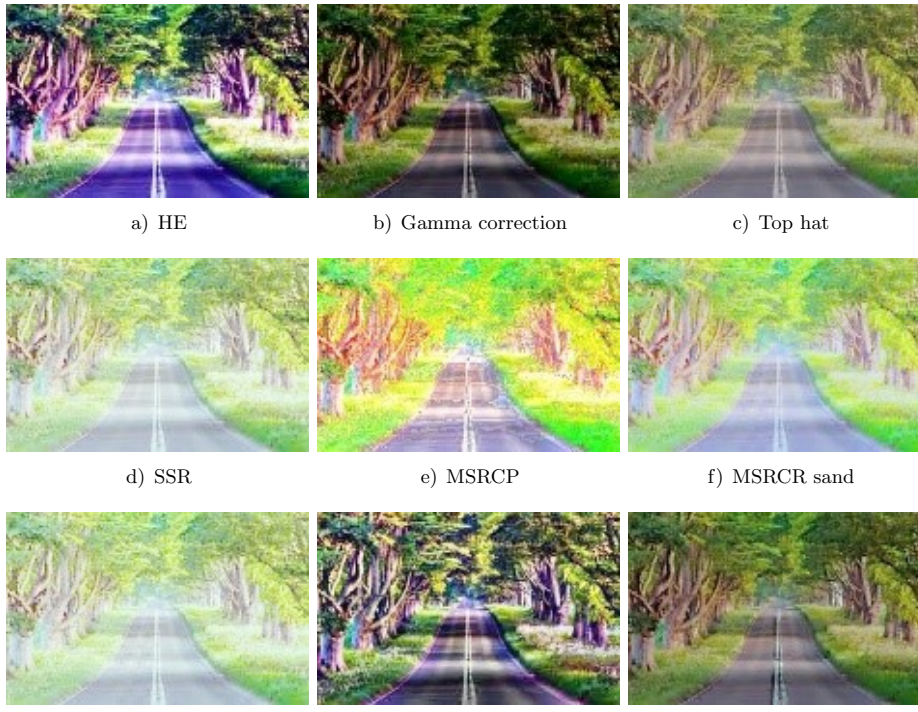

a) HE b) Gamma correction c) Top hat

d) SSR e) MSRCP f) MSRCR sand

g) MSR h) CLAHE i) Proposed algorithm

Figure 11. Various algorithms to enhance the forest path imag

Figures 11, 12 and 13 show the processing effect of different algorithms on three different kinds of pictures. The enhanced image clearly shows that the algorithm can not only adjust the brightness of the image, but also enhance the detailed features of the image to ensure that the image is not distorted. From the enhanced image in Figure 11, it is evident that the textural details of the trees and the color changes of the distant roads are clear and discernable. Similarly, the distant doors and windows are easily identifiable and the street lights are brightened to a suitable level after the enhancement of the images of the urban nightscape in Figure 12. For the landscape images, the details of the buildings and mountains have evidently become more distinct, as shown in Figure 13.

To compare the effect of another image enhancement algorithm more directly with that of our proposed algorithm, Table 1, 2 and 3 respectively compare the structural similarity (SSIM), peak signal to noise ratio (PSNR) and mean square error (MSE) as evaluation indexes, where the processing effects of each algorithm on three images are compared. The algorithms involved in the comparison are:

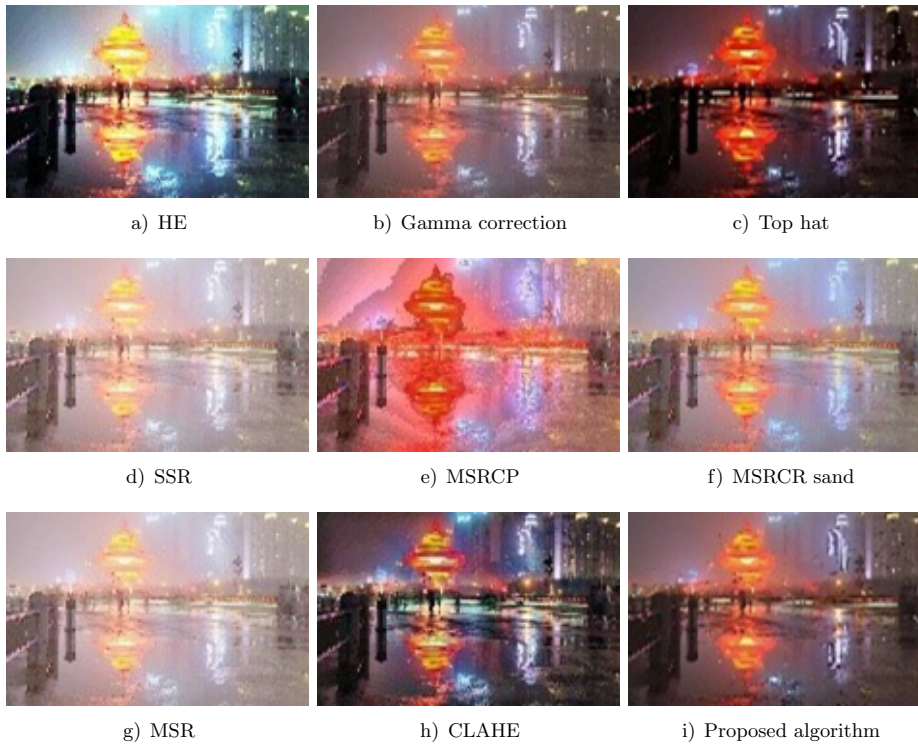

a) HE b) Gamma correction c) Top hat

d) SSR e) MSRCP f) MSRCR sand

g) MSR h) CLAHE i) Proposed algorithm

Figure 12. Various algorithms to used to enhance the urban nightscape image

HE [25] (Histogram Equalization), Gamma correction [16], Top hat [19], SSR [5], MSRCP [26] (Multi-scale Retinex with chromaticity preservation), MSRCR [18], MSR [19], CLAHE [27] (Contrast Limited Adaptive Histogram Equalization).

For the forest road image, as the overall color is more vivid, we can see from Table 1 that the SSIM values of other algorithms are low. This shows that in the original, brightly colorful image, the contrast algorithm does not enhance the image. For urban nightscape images, the details of windows, pedestrians, streetlights and distant tall buildings are the key to evaluating enhancement. Observing the results in Table 1, the SSIM values of each algorithm are relatively close, including top hat algorithm, gamma correction and this new algorithm. The enhancement effect of the top hat algorithm is more serious on a subjective level, and at the same time, the color and brightness of the image are not enhanced. For the landscape images, the difficulty of enhancement lies in the architecture of the distant view and the sky behind the mountain. A comparison of the SSIM values of the algorithms in Table 1, and the proposed algorithm appear to have a better visual rendering effect. By visual inspection, we can see that beyond the algorithm proposed in this paper, the index values of other algorithms are relatively high when processing the land-

	HE	Gamma Correction	Top Hat	SSR	MSRCP	MSRCR	MSR	CLAHE	Proposed Algorithm
Forest path image	0.7201	0.8487	0.8910	0.6262	0.4449	0.6212	0.6179	0.6671	0.9283
Urban nightscape image	0.7014	0.8196	0.8531	0.5911	0.5063	0.6506	0.5959	0.7913	0.9437
Landscape image	0.8401	0.9097	0.9217	0.9153	0.9428	0.8717	0.8659	0.8429	0.953

Table 1. Comparison of the structural similarity (SSIM) between different image enhancement algorithms and the proposed algorithm

	HE	Gamma Correction	Top Hat	SSR	MSRCP	MSRCR	MSR	CLAHE	Proposed Algorithm
Forest path image	13.6237	14.3032	26.3223	7.4964	7.7319	8.4513	7.5849	14.6509	26.9733
Urban nightscape image	11.6390	14.7244	24.7538	8.1254	10.3273	10.1847	8.3188	18.8805	28.1815
Landscape image	16.5730	16.9717	26.2814	16.0936	19.7034	17.0164	16.4805	22.3985	29.4409

Table 2. Comparison of the peak signal to noise ratio (PSNR) between different image enhancement algorithms and the proposed algorithm

	HE	Gamma Correction	Top Hat	SSR	MSRCP	MSRCR	MSR	CLAHE	Proposed Algorithm
Forest path image	2 823.0	2 414.1	160.4	11 573	10 962	9 288.5	11 339	2 228.4	130.5
Urban nightscape image	4 458.4	2 191.0	293.2	10 013	6 030.5	6 231.7	9 576.3	855.5	188.4
Landscape image	1 431.5	1 305.9	153.1	1 598.5	696.2	1 292.5	1 462.3	374.3	139.6

Table 3. Comparison of the mean square error (MSE) between different image enhancement algorithms and the proposed algorithm

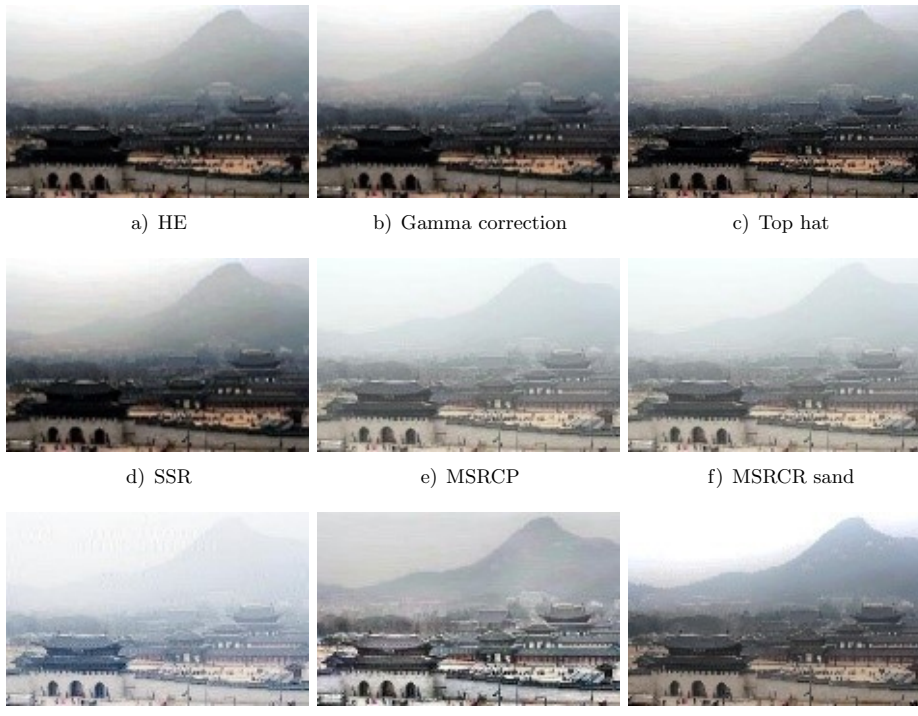

a) HE b) Gamma correction c) Top hat

d) SSR e) MSRCP f) MSRCR sand

g) MSR h) CLAHE i) Proposed algorithm

Figure 13. Various algorithms for the landscape image enhancement

scape image. However, the SSIM values of this algorithm are higher when the forest path image and the urban nightscape image are processed, and the SSIM values are used when the landscape images are processed. The algorithm can maintain a relatively consistent enhancement effect in three different scenarios. Other image enhancement algorithms exhibit certain limitations in their application and cannot be used across a variety of scenarios. These limitations include poor overall image enhancement and balance, as well as limited localized enhancement. Additionally, some algorithms aim to restore the overall color, while others focus on high frequency partial enhancement. All of these problems can be solved by the proposed algorithm.

By comparing the PSNR index, it can be seen from Table 2 that in the forest path image, the algorithm of this paper is equivalent to the top hat algorithm, but in the urban nightscape image and the landscape image, the algorithm of this paper is better than the top hat algorithm. In the landscape image, the proposed algorithm is slightly higher than the CLAHE algorithm, but the effect on the other two images is far less than the algorithm in this paper. In addition, comprehensively comparing other several algorithms, the effect of the proposed algorithm is much better than

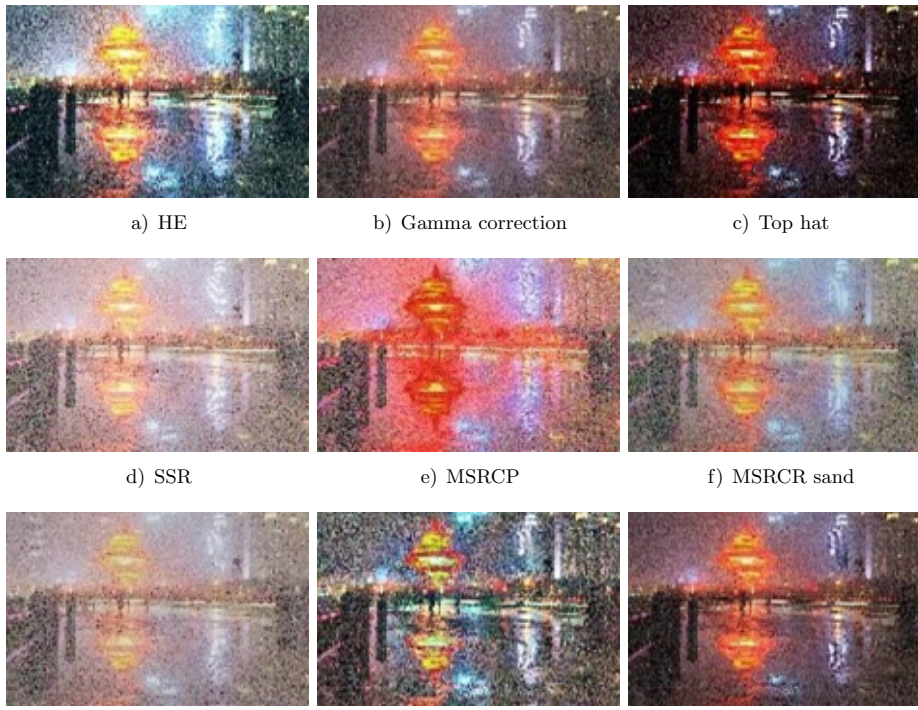

a) HE b) Gamma correction c) Top hat

d) SSR e) MSRCP f) MSRCR sand

g) MSR h) CLAHE i) Proposed algorithm

Figure 14. Different algorithms on Gaussian noise

the others. After each algorithm processes the three images separately, it is found that the algorithm has the best enhancement effect on the landscape image. The proposed algorithm has the same effect for image enhancement in the three scenarios and has stronger generalization ability.

The numerical comparison of the mean square error index of the natural image in the proposed algorithm is shown in Table 3. This comparison index is different from SSIM, whereby a high value indicates a low quality picture. The results in Table 3 show that the all three methods (CLAHE, top hat and the algorithm of this paper) enhance the image with good results. Although the SSIM values of our algorithm and the top hat enhancement algorithm are similar in the enhancement of the landscape image, the image enhancement effect of the top hat algorithm is much lower than that of the proposed algorithm, demonstrating the stability of our algorithm in dealing with different images.

To demonstrate the robustness of the proposed algorithm, noise and contrast are added to the image and experiments on the image enhancement ability were performed. A series of other noises such as speckle noise, Poisson noise, Gaussian noise, salt and pepper noise are detected, as shown in Figures 14, 15, 16 and 17.

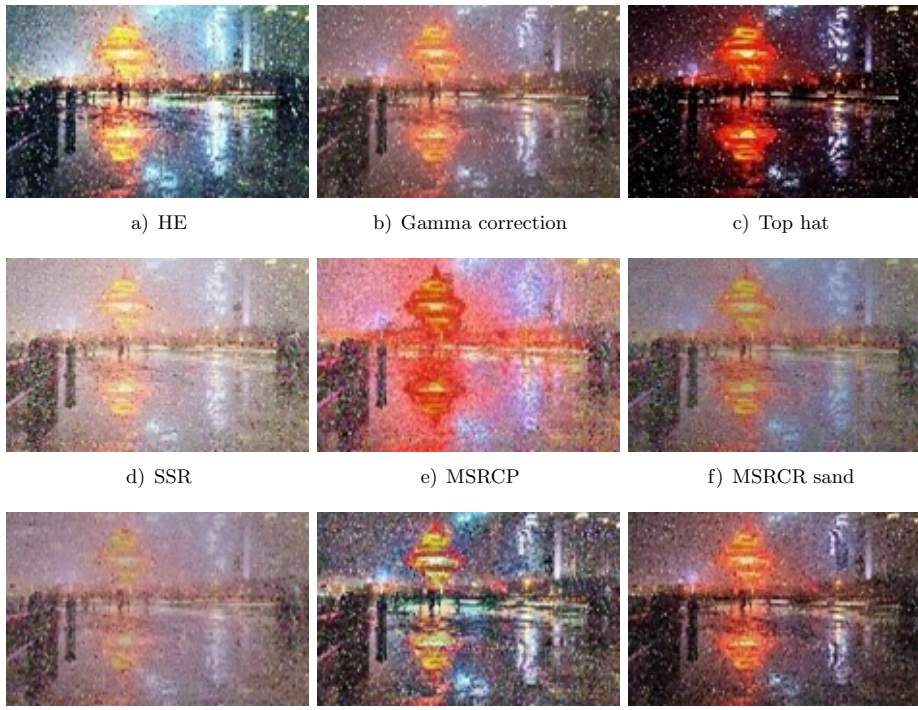

a) HE b) Gamma correction c) Top hat

d) SSR e) MSRCP f) MSRCR sand

g) MSR h) CLAHE i) Proposed algorithm

Figure 15. Different algorithms on the treatment of salt and pepper noise

The structural similarity (SSIM), peak signal-to-noise ratio (PSNR), and mean square error (MSE) of the image are highlighted in Figure 18. The noise data in the image is randomly assigned during the calculation of these values. Due to the need for objective values, 32 image tests were performed in this study, and their values summed to obtain the average value for comparison. From Figure 18 a), the PSNR of the algorithms in the processing of four kinds of noise can be seen. The higher value indicates that the proposed algorithm has good robustness and can suppress noise interference while enhancing the image. As Figure 18 shows, each algorithm of the top hat enhancement algorithm contains various noises. The result of image processing is in line with the expected outcome, although the index of the algorithm is high. The analysis concludes that the top hat enhances the edge of the image through the expansion and erosion of the image which results in the strengthening of the image at the edges. The low frequency part does not have the corresponding enhancement operation, and the top hat algorithm has less advantages than this one. Although the proposed algorithm achieves a good denoising effect for different noises, the processing mechanism is also different and the removal of Poisson noise is better than other types of noise.

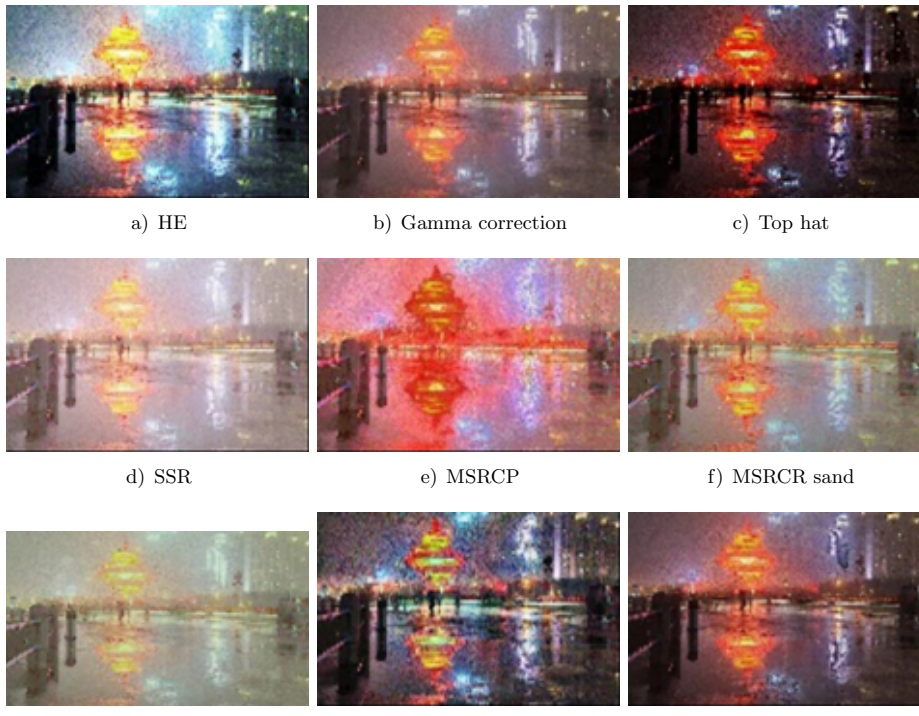

a) HE b) Gamma correction c) Top hat

d) SSR e) MSRCP f) MSRCR sand

g) MSR h) CLAHE i) Proposed algorithm

Figure 16. Different algorithms for the treatment of speckle noise

5 CONCLUSION

Aiming at the problems of the existing image enhancement algorithms with large limitations and poor adaptability, this paper proposes an image enhancement algorithm based on the image spatial domain segmentation. The standard deviation of the mathematical function is used to establish a mathematical model based on the correspondence between the spatial domain and the frequency, and a 3×3 receptive field is designed through a two-dimensional Gaussian function, and Gaussian proportional weight distribution is performed. According to the difference between the pixels in the image, the image is divided into four frequency regions: low frequency, low-medium frequency, medium-high frequency and high frequency. The methods of gamma correction, MSRCR, MSR and top hat + bottom hat are used to enhance them by region respectively. Then the enhanced regional images are merged, and the resulting enhanced image has a higher image quality. The three indicators of PSNR, SSIM, and MSE are used to evaluate the image quality. The experimental results show that the image enhancement algorithm proposed in this paper is superior to other algorithms and can retain image details more

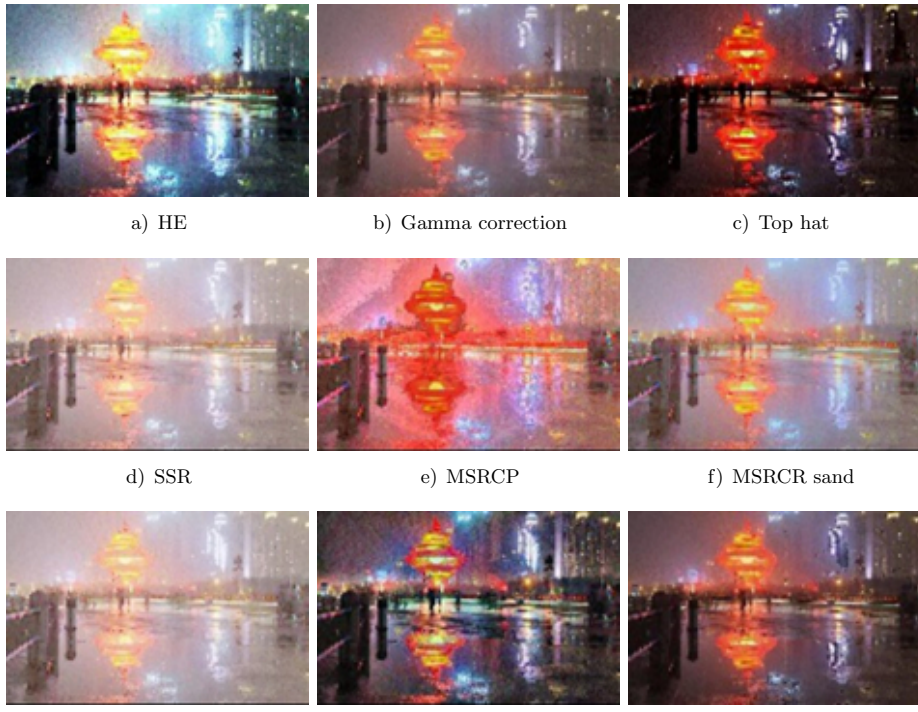

a) HE b) Gamma correction c) Top hat

d) SSR e) MSRCP f) MSRCR sand

g) MSR h) CLAHE i) Proposed algorithm

Figure 17. Different algorithms for Poisson noise processing

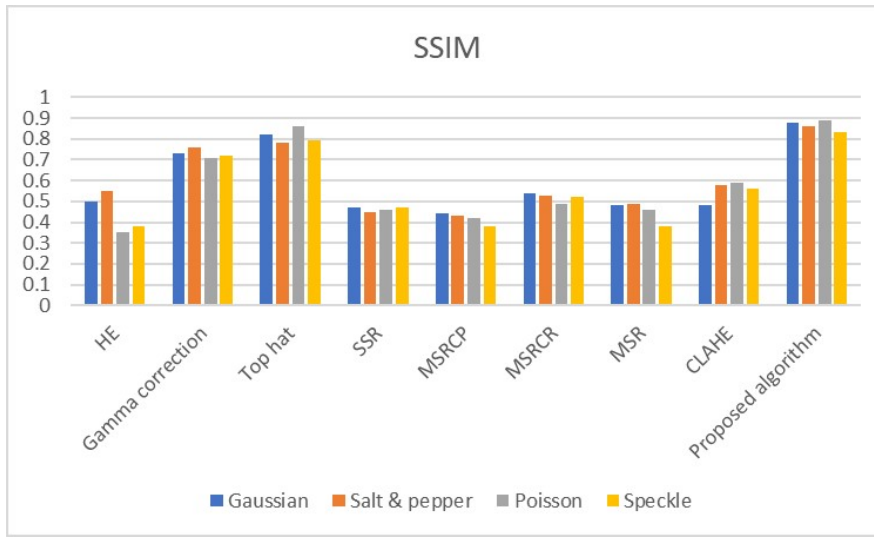

a) SSIM

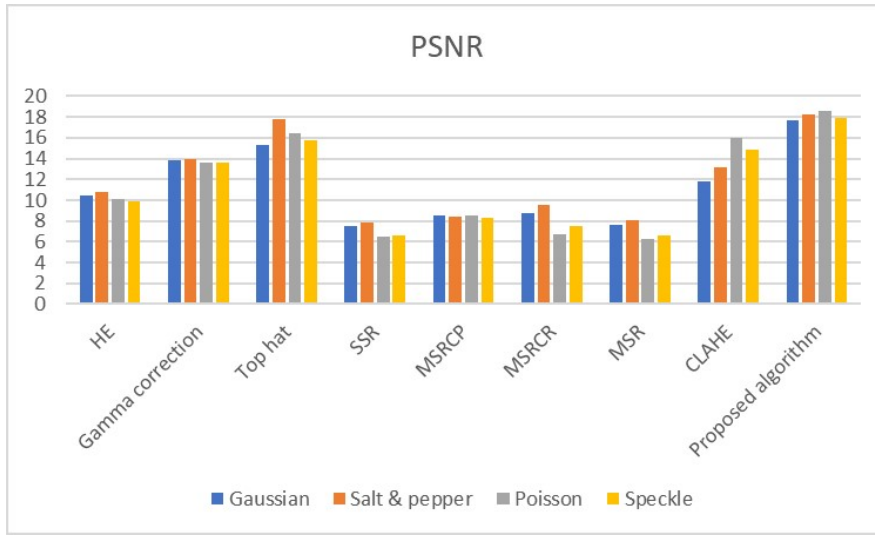

b) PSNR

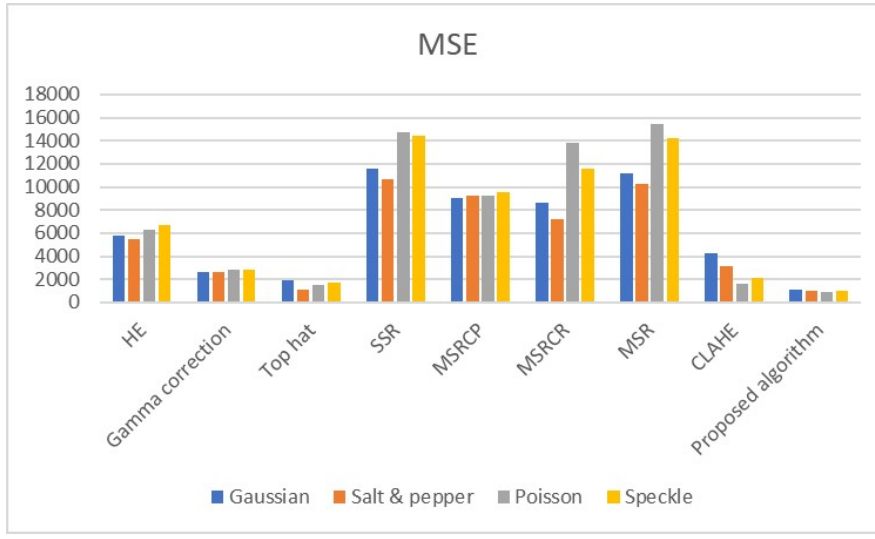

c) MSE

Figure 18. Comparison of the SSIM, PSNR and MSE indices of the different algorithms tested following the addition of various types of noise (Gaussian, salt and pepper, Poisson, speckle)

effectively, which proves the effectiveness and superiority of the algorithm in this paper.

REFERENCES

[1] Lu, D. G.—Geng, P.—He, H. X.—Wang, P. P.: Application of Low Illuminance Image Enhancement Based on Improved Retinex Algorithm in Urban Utility Tunnel. International Core Journal of Engineering, Vol. 5, 2019, No. 8, pp. 190–197.

[2] McCann, J.: Retinex Theory. In: Luo, M. R. (Ed.): Encyclopedia of Color Science and Technology. Springer, New York, 2016, doi: 10.1007/978-1-4419-8071-7_260.

[3] Hussein, R. R.—Hamodi, Y. I.—Sabri, R. A.: Retinex Theory for Color Image Enhancement: A Systematic Review. International Journal of Electrical and Computer Engineering (IJECE), Vol. 9, 2019, pp. 5560–5569, doi: 10.11591/ijece.v9i6.pp5560-5569.

[4] Qu, J. H.—Li, Y. S.—Du, Q.—Dong, W. Q.—Xi, B. B.: Hyperspectral Pansharpening Based on Homomorphic Filtering and Weighted Tensor Matrix. Remote Sensing, Vol. 11, 2019, No. 9, Art. No. 1005, doi: 10.3390/rs11091005.

[5] Sun, Q. J.—Jiang, H. Y.—Yi, D. H.: A Study of Pathological Image Detail Enhancement Method Based on Improved Single Scale Retinex. Journal of Medical Imaging and Health Informatics, Vol. 8, 2018, No. 5, pp. 1051–1056, doi: 10.1166/jmihi.2018.2396.

[6] Liu, X.—Xia, X. H.—Wang, L.—Cao, J. H.: Color Image Enhancement Based on Adaptive Multi-Scale Morphological Unsharpening Filter. IOP Conference Series: Materials Science and Engineering, Vol. 423, 2018, No. 1, Art. No. 012082, doi: 10.1088/1757-899X/423/1/012082.

[7] Liu, Y. H.—Yan, H. M.—Gao, S. B.—Yang, K. F.: Criteria to Evaluate the Fidelity of Image Enhancement by MSRCR. IET Image Processing, Vol. 12, 2018, No. 6, pp. 880–887, doi: 10.1049/iet-ipr.2017.0171.

[8] Wang, Z. J.—Luo, Y. Y.—Jiang, S. Z.—Xiong, N. F.—Wan, L. T.: An Improved Algorithm for Adaptive Infrared Image Enhancement Based on Guided Filtering. Spectroscopy and Spectral Analysis, Vol. 40, 2020, No. 11, pp. 3463–3467 (in Chinese).

[9] Han, M. Y.—Li, L. G.—Jiang, K.: Retinex Low-Illumination Image Enhancement Algorithm Based on Light Image Estimation. Computer Engineering, Vol. 47, 2021, No. 10, pp. 201–206,, doi: 10.19678/j.issn.1000-3428.0059224 (in Chinese).

[10] Lan, R.—Jia, Y. W.: Adaptive Intuitionistic Fuzzy Dissimilar Histogram Clipping Image Enhancement Algorithm. Control and Decision, Vol. 36, 2021, No. 12, pp. 2919–2928, doi: 10.13195/j.kzyjc.2020.0845 (in Chinese).

[11] Cao, L. X.—Ma, Z. F.—Shi, J.: Retinex-Based Adaptive Non-Uniform Low Light Image Enhancement Algorithm. Computer Measurement and Control, Vol. 28, 2020, No. 10, pp. 155–159 (in Chinese).

[12] Cai, X. M.—Ma, J. L.—Wu, C. M.—Xue, H.: Color Image Enhancement Algorithm Based on Fuzzy Homomorphic Filtering. Computer Simulation, Vol. 37, 2020, No. 6, pp. 342–346 (in Chinese).

[13] Valero, E. M.—Nieves, J. L.—Hernández-Andrés, J.—García, J. A.: Changes in Contrast Thresholds with Mean Luminance for Chromatic and Luminance Gratings: A Reexamination of the Transition from the DeVries-Rose to Weber Regions. Color Research and Application, Vol. 29, 2004, No. 3, pp. 177–182, doi: 10.1002/col.20003.

[14] Maruyama, S.: Visualization of Blurring Process Due to Analog Components in a Digital Radiography System Using a Simple Method. Physical and Engineering Sciences in Medicine, Vol. 43, 2020, No. 4, pp. 1461–1468, doi: 10.1007/s13246-020-00939-3.

[15] Kim, D.: Performance Analysis of Retinex-Based Image Enhancement According to Color Domain and Gamma Correction Adaptation. Journal of Korea Society of Digital Industry and Information Management, Vol. 15, 2019, No. 1, pp. 99–107, doi: 10.17662/KSDIM.2019.15.1.099.

[16] Ashiba, M. I.—Tolba, M. S.—El-Fishawy, A. S.—Abd El-Samie, F. E.: Gamma Correction Enhancement of Infrared Night Vision Images Using Histogram Processing. Multimedia Tools and Applications, Vol. 78, 2019, No. 19, pp. 27771–27783, doi: 10.1007/s11042-018-7086-y.

[17] Song, X.—Xiong, S. H.—He, X. H.—Kang, P. X.: Retinex Enhancement Algorithm for Low Intensity Images Based on HSI Space. Journal of Image and Signal Processing, Vol. 6, 2017, No. 1, pp. 29–36, doi: 10.12677/jisp.2017.61004 (in Chinese).

[18] Ma, J. X.—Fan, X. N.—Ni, J. J.—Zhu, X. F.—Xiong, C.: Multi-Scale Retinex with Color Restoration Image Enhancement Based on Gaussian Filtering and Guided Filtering. International Journal of Modern Physics B, Vol. 31, 2017, No. 16–19, Art. No. 1744077, doi: 10.1142/S0217979217440775.

[19] Swathika, R.—Sharmila, T. S.: Image Fusion for MODIS and Landsat Images Using Top Hat Based Moving Technique with FIS. Cluster Computing, Vol. 22, 2019, No. 5, pp. 12939–12947, doi: 10.1007/s10586-018-1802-2.

[20] Bommisetty, R. M.—Prakash, O.—Khare, A.: Video Superpixels Generation Through Integration of Curvelet Transform and Simple Linear Iterative Clustering. Multimedia Tools and Applications, Vol. 78, 2019, No. 17, pp. 25185–25219, doi: 10.1007/s11042-019-7554-z.

[21] Tang, D.—Fu, H.—Cao, X.: Topology Preserved Regular Superpixel. 2012 IEEE International Conference on Multimedia and Expo, Melbourne, VIC, Australia, 2012, pp. 765–768, doi: 10.1109/ICME.2012.184.

[22] Achanta, R.—Shaji, A.—Smith, K.—Lucchi, A.—Fua, P.—Süsstrunk, S.: SLIC Superpixels Compared to State-of-the-Art Superpixel Methods. IEEE Transactions on Pattern Analysis and Machine Intelligence, Vol. 34, 2012, No. 11, pp. 2274–2282, doi: 10.1109/TPAMI.2012.120.

[23] Kovesi, P.: Image Segmentation Using SLIC Superpixels and DBSCAN Clustering. University of Western Australia. Center for Exploration Targeting, Image Analysis Group, Vol. 7, 2013.

[24] Jia, S.—Geng, S.—Gu, Y.—Yang, J.—Shi, P.—Qiao, Y.: NSLIC: SLIC Superpixels Based on Nonstationarity Measure. 2015 IEEE International Conference on Image Processing (ICIP), 2015, pp. 4738–4742, doi: 10.1109/ICIP.2015.7351706.

[25] Mayathevar, K.—Veluchamy, M.—Subramani, B.: Fuzzy Color Histogram Equalization with Weighted Distribution for Image Enhancement. Optik, Vol. 216, 2020, Art. No. 164927, doi: 10.1016/j.ijleo.2020.164927.

[26] Heng, B. C.—Xiao, D.—Zhang, X.: Night Color Image Mosaic Algorithm Combined with MSRCP. Computer Engineering and Design, Vol. 40, 2019, No. 11, pp. 3200–3204 (in Chinese).

[27] Fu, Q. Q.—Celenk, M.—Wu, A. P.: An Improved Algorithm Based on CLAHE for Ultrasonic Well Logging Image Enhancement. Cluster Computing, Vol. 22, 2019, No. 5, pp. 12609–12618, doi: 10.1007/s10586-017-1692-8.

Tianhe Yu is Professor in the Harbin University of Science and Technology. His main research fields are information and signal processing, image enhancement and recognition.

Ming Zhu works in the Harbin University of Science and Technology. Her main research fields are deep learning and image processing.